

Axionic dark matter signatures in various halo models

, J.D. Vergados^{1,2} and Y. Semertzidis¹

*1 KAIST University, Daejeon, Republic of Korea and
Center for Axion and Precision Physics Research, IBS, Daejeon 305-701, Republic of Korea
ARC Centre of Excellence in Particle Physics at the Terascale and Centre for the Subatomic
Structure of Matter (CSSM), University of Adelaide, Adelaide SA 5005, Australia^{#1}*

Abstract

In the present work we study possible time signatures Axion Dark Matter searches employing resonant cavities for various halo models. We study in particular the time dependence of the resonance width (modulation) and possible asymmetries in directional experiments.

1. Introduction

The axion has been proposed a long time ago as a solution to the strong CP problem [1] resulting to a pseudo Goldstone Boson [2, 3, 4, 5, 6], but it has also been recognized as a prominent dark matter candidate [7]. In fact, realizing an idea proposed a long time ago by Sikivie [8], various experiments such as ADMX and ADMX-HF collaborations [9, 10], [11],[12] are now planned to search for them. In addition, the newly established center for axion and physics research (CAPP) has started an ambitious axion dark matter research program [13], using SQUID and HFET technologies [14]. The allowed parameter space [15], containing information for all the axion like particles, defines a region for invisible axions, which can be dark matter candidates.

In the present work we will assume that the axion is non relativistic with mass in μeV - meV scale, moving with an average velocity which is $\approx 0.8 \times 10^{-3}c$. It is expected to be observed in resonance cavities with a width that depends on the axion mean square velocity in the local frame. The latter depends on the assumed halo model. We will expand and improve our previous work [16, 17] by including various popular halo models. We will study the time variation of the width due to the motion of the Earth around the sun and possible asymmetries with regard to the sun's direction of motion as it goes around the center of the galaxy. Due to the rotation of the Earth around its axis these asymmetries in

^{#1}Physics Department, Univesity of Ioannina. e-mail:vergados@uoi.gr

the width of the resonance will manifest themselves in their diurnal variation. These important signatures may become more needed, if indeed the predicted axion to photon coupling becomes weaker as some recent models predict [18].

2. Brief summary of the formalism

The photon axion interaction is dictated by the Lagrangian:

$$\mathcal{L}_{a\gamma\gamma} = g_{a\gamma\gamma} a \mathbf{E} \cdot \mathbf{B}, \quad g_{a\gamma\gamma} = \frac{\alpha g_\gamma}{\pi f_a}, \quad (2.1)$$

where \mathbf{E} and \mathbf{B} are the electric and magnetic fields, g_γ a model dependent constant of order one [9],[19][20] and f_a the axion decay constant. Axion dark matter detectors [19] employ an external magnetic field, $\mathbf{B} \rightarrow \mathbf{B}_0$ in the previous equation, in which case one of the photons is replaced by a virtual photon, while the other maintains the energy of the axion, which is its mass plus a small fraction of kinetic energy.

The power produced, see e.g. [9], is given by:

$$P_{mnp} = g_{a\gamma\gamma}^2 \frac{\rho_a}{m_a} B_0^2 V C_{mnp} Q_L \quad (2.2)$$

Q_L is the loaded quality factor of the cavity. Here we have assumed Q_L is smaller than the axion width Q_a , see below. More generally, Q_L should be substituted by $\min(Q_L, Q_a)$. This power depends on the axion density and is pretty much independent of the velocity distribution.

The axion power spectrum, which is of great interest to experiments, is written as a Breit-Wigner shape [19], [21]:

$$|\mathcal{A}(\omega)|^2 = \frac{\rho_D}{m_a^2} \frac{\Gamma}{(\omega - \omega_a)^2 + (\Gamma/2)^2}, \quad \Gamma = \frac{\omega_a}{Q_a} \quad (2.3)$$

Since in the axion DM search case the cavity detectors have reached such a very high energy resolution [22, 23], one should try to accurately evaluate the width of the expected power spectra in various theoretical models.

3. Evaluation of the width in the local frame

We will derive the expression for the width assuming in the galactic frame a Maxwell Boltzmann axion velocity distribution:

$$f(v) = \frac{1}{\pi\sqrt{\pi}} \frac{1}{v_0^3} e^{-\frac{v^2}{v_0^2}} \quad (3.4)$$

We will use the relation

$$\omega = m_a \left(1 + \frac{1}{2} v^2 \right) \quad (3.5)$$

or

$$v = \sqrt{\frac{2(\omega - m)}{m}}, v dv = \frac{d\omega}{m}$$

In the galactic frame the number of axions in the with frequency between ω and $\omega + d\omega$ in a solid angle $d\Omega$ is

$$dN_a = \frac{\rho_a}{m_a} \frac{1}{\pi\sqrt{\pi}} \frac{1}{v_0^3} e^{-2\frac{\omega-m}{mv_0^2}} \sqrt{\frac{2(\omega-m)}{m}} \frac{d\omega}{m} d\Omega \quad (3.6)$$

Introducing the variable $x = 2\frac{\omega-m}{mv_0^2}$ we find:

$$dN_a = \frac{\rho_a}{m_a} g(x) \frac{d\Omega}{4\pi}, g(x) = \frac{2}{\sqrt{\pi}} \sqrt{x} e^{-x} \quad (3.7)$$

The maximum of the distribution occurs at $x = 1/2$. The width at half maximum is $\delta x = x_2 - x_1$ with x_i the roots of the equation

$$g(x) = \frac{1}{2} g(x)|_{x=1/2} \Rightarrow \sqrt{x} e^{-x} = \frac{1}{2\sqrt{2}} e^{-\frac{1}{2}}$$

We thus find $\delta x = 1.8$. Thus the width at half maximum in frequency space is:

$$\delta\omega = m \frac{1}{2} v_0^2 \delta x \Rightarrow \frac{1}{Q_a} = \frac{1}{2} v_0^2 \delta x = \delta x \frac{1}{3} \prec v^2 \succ_g \quad (3.8)$$

where the last quantity is the average of the square of the axion velocity in the galactic frame.

Our next task is to transform the velocity distribution from the galactic to the local frame. The needed equation, see e.g. [24], is:

$$\mathbf{y} \rightarrow \mathbf{y} + \hat{v}_s + \delta (\sin \alpha \hat{x} - \cos \alpha \cos \gamma \hat{y} + \cos \alpha \sin \gamma \hat{v}_s), \quad y = \frac{v}{v_0} \quad (3.9)$$

with $\gamma \approx \pi/6$, \hat{v}_s a unit vector in the Sun's direction of motion, \hat{x} a unit vector radially out of the galaxy in our position and $\hat{y} = \hat{v}_s \times \hat{x}$. The last term in the first expression of Eq. (3.9) corresponds to the motion of the Earth around the Sun with δ being the ratio of the modulus of the Earth's velocity around the Sun divided by the Sun's velocity around the center of the Galaxy, i.e. $v_0 \approx 220\text{km/s}$ and $\delta \approx 0.135$. The above formula assumes that the motion of both the Sun around the Galaxy and of the Earth around the Sun are uniformly circular. The exact orbits are, of course, more complicated but such deviations are not expected to significantly modify our results. In Eq. (3.9) α is the phase of the Earth ($\alpha = 0$ around the beginning of June)².

²One could, of course, make the time dependence of the rates due to the motion of the Earth more explicit by writing $\alpha \approx (6/5)\pi (2(t/T) - 1)$, where t/T is the fraction of the year.

In the local frame, ignoring the motion of the Earth, we make in the velocity distribution the substitution:

$$v^2 \rightarrow v^2 + v_0^2 + 2vv_0\xi, \quad \xi = \hat{v} \cdot \hat{v}_z$$

where v_0 is the speed of the sun around the center of the galaxy and \hat{v}_z , is a unit vector in the sun's direction of motion. Thus Eq. (3.7)

$$dN_a = \frac{\rho_a}{m_a} g(x, \xi) \frac{d\Omega}{4\pi}, \quad g(x, \xi) = \frac{2}{\sqrt{\pi}} \sqrt{x} e^{-(1+x+2\xi\sqrt{x})} \quad (3.10)$$

The function $g(x, \xi)$ is exhibited in Fig. 3.1.

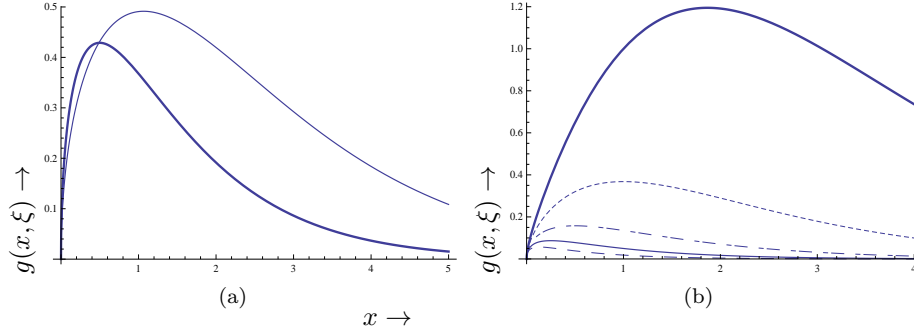


Figure 3.1: The function $g(x, \xi)$, $x = 2\frac{\omega-m}{mv_0^2}$, which essentially gives the normalized frequency distribution, is exhibited. In (a) we show the distribution in the galactic frame (thick solid line) and its angle average in the local frame (solid line). In (b) we exhibit the angular dependence of the distribution in the local frame for some typical values of ξ , $x\xi = \cos\theta$, θ being the polar angle of the velocity with respect to the sun's direction of motion. The motion of the Earth is ignored. From top to bottom $\xi = -1, -1/2, 0, 1/2, 1$. The asymmetry is obvious.

$g(x, \xi)$ has extrema at

$$x = \left\{ \frac{1}{2} \left(\xi^2 - \sqrt{\xi^4 + 2\xi^2 + 1} \right), \frac{1}{2} \left(\xi^2 + \sqrt{\xi^4 + 2\xi^2 + 1} \right) \right\}$$

The first of these yields a maximum for all ξ , while the second is the location of a maximum only for $-1 \leq \xi \leq \frac{1}{4}\sqrt{19 - 3\sqrt{33}} = 0.33$.

Clearly the width at half maximum is a function of ξ . Its value is obtained numerically and it is exhibited in Fig. 3.2a,b, corresponding to whether the

sense of direction of the axion can be determined or not. The width clearly has a maximum opposite to the sun's direction of motion (a), if the sense of direction of the axion can be determined, something perhaps not very realistic. It exhibits simply a minimum in the plane perpendicular to the sun's velocity, in the most realistic scenario that the sense of direction cannot be determined (b).

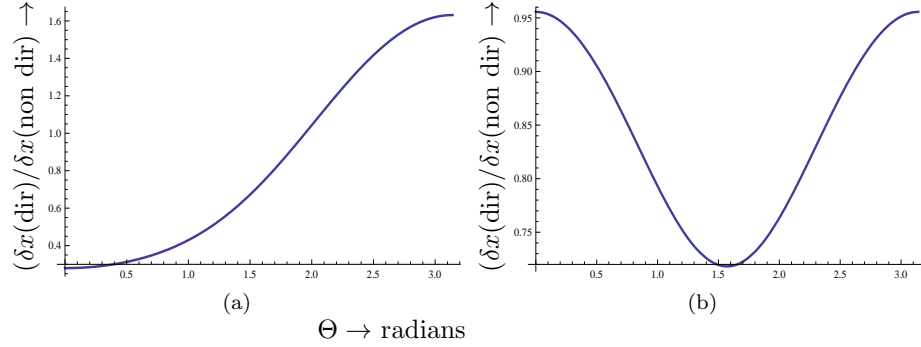


Figure 3.2: The width δx expected in directional experiments, relative to that of the standard (non directional) experiments, as a function of the polar angle with sense of direction known (a) and with sense of direction not known (b).

We will next consider the effect of the Earth's motion in the standard, non directional, experiments. The azimuthal angle (ϕ) dependence, averages out to zero. Thus the distribution takes the form:

$$dN_a = \frac{\rho_a}{m_a} h(x, \xi, \cos \alpha) \frac{d\Omega}{4\pi}, \quad h(x, \xi, \cos \alpha) = \frac{2}{\sqrt{\pi}} \sqrt{x} e^{-(1+x+(2+\delta \cos \alpha)\xi\sqrt{x})} \quad (3.11)$$

$$g(x, \cos \alpha) = \int h(x, \xi, \cos \alpha) \frac{d\Omega}{4\pi} = \frac{2e^{-x-1} \sinh(\sqrt{x}(\delta \cos(\alpha) + 2))}{\sqrt{\pi} \sqrt{x}(\delta \cos(\alpha) + 2)}$$

The maximum of the distribution $g(x, \cos \alpha)$ occurs at the root $r_1(\cos \alpha)$ of the equation :

$$\coth(\sqrt{x}(\delta \cos(\alpha) + 2)) - \frac{\sqrt{x}}{\delta \cos(\alpha) + 2} = 0$$

which is obtained graphically. Then $\delta x(\cos \alpha) = x_2(\cos \alpha) - x_1(\cos \alpha)$ where $x_1(\cos \alpha)$ and $x_2(\cos \alpha)$ are the roots of the equation:

$$g(x, \cos \alpha) = (1/2)g(r_1(\cos \alpha), \cos \alpha)$$

where

$$g(x, \cos \alpha) = \sqrt{x} e^{-(1+x+(2+\delta \cos \alpha)\xi\sqrt{x})}$$

The obtained results are exhibited in Fig. 3.3.

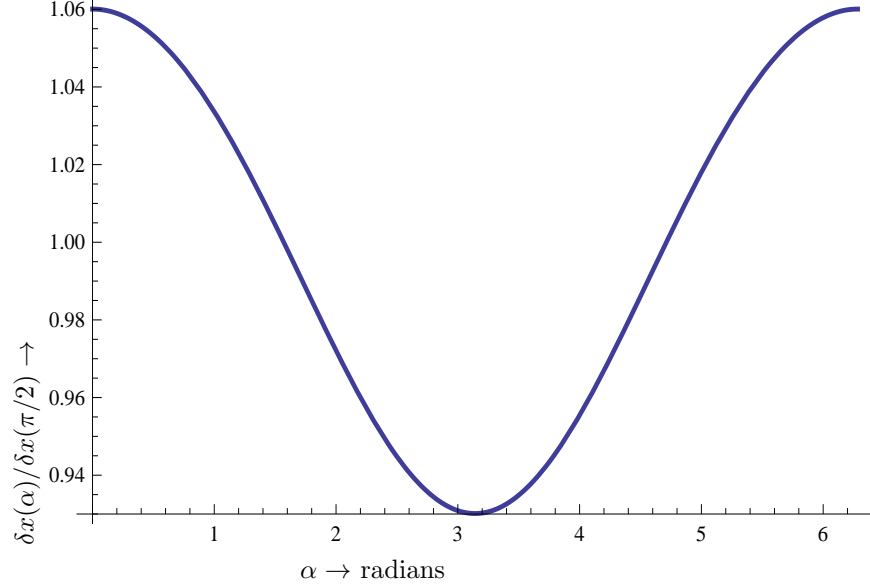


Figure 3.3: The modulated width δx , relative to its time average, as a function of the phase of the Earth α ($\alpha = 0$ on June 3rd).

4. More complicated velocity distributions

In the context of dark matter other velocity distributions have been considered, e.g. completely phase-mixed DM, dubbed “debris flow” (Kuhlen et al. [25]) and caustic rings (Sikivie [26],[27][28], Vergados [29]).

4.1. The case of debris flows

In the case of debris flows one assumes a dark matter distribution which is of the form:

$$f(v) = (1 - \epsilon(\zeta))f_{MB}(v) + \epsilon(\zeta)f_{db}(v) \quad (4.12)$$

with

$$f_{db}(v) = \begin{cases} \frac{1}{2v_f v_0} v, & v_f - v_0 \leq v \leq v_f + v_0 \\ 0 & \text{otherwise} \end{cases} \quad (4.13)$$

where

$$\epsilon(\zeta) = 0.22 + 0.34 \left(\text{erf} \left(\zeta \frac{220}{185} - \frac{465}{185} \right) + 1 \right) \quad (4.14)$$

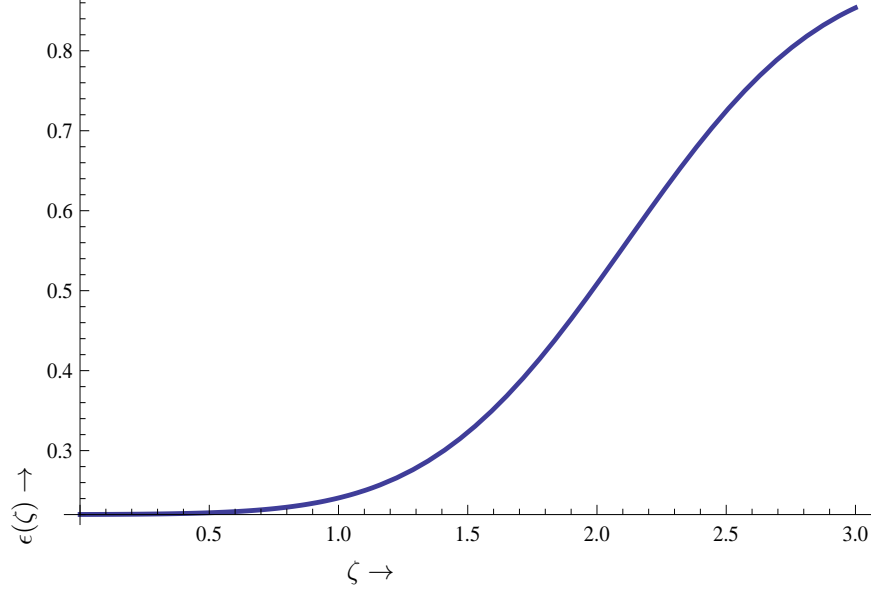


Figure 4.4: The amplitude $\epsilon(\zeta)$ entering the debris flow component of dark matter. Of particular interest is the region of ζ between 1.5 and 2.

The introduction of debris flows has two effects:

- It shifts the maximum of the distribution, without changing the location of the maximum r_1 .

$$g(x) \rightarrow (1 - \epsilon(\zeta))g(x) + \epsilon(\zeta)g_{df}(x) \quad (4.15)$$

with

$$g_{df}(x) = \begin{cases} \frac{1}{4(1+\zeta)}, & \zeta^2 \leq x \leq (2+\zeta)^2 \\ 0 & \text{otherwise} \end{cases} \quad (4.16)$$

- The width at half maximum is affected:

$$g(x) = \frac{1}{2}g(r_1) \Leftrightarrow (1 - \epsilon(\zeta))g(x) + \epsilon(\zeta)g_{df}(x) = (1 - \epsilon(\zeta))g(r_1) + \epsilon(\zeta)g_{df}(r_1) \quad (4.17)$$

We thus find:

- In the galactic frame:

$\delta x = (1.82, 1.81, 1.97, 2.11, 2.40)$ for $\epsilon = (0.220, 0.222, 0.241, 0.323, 0.508)$ respectively

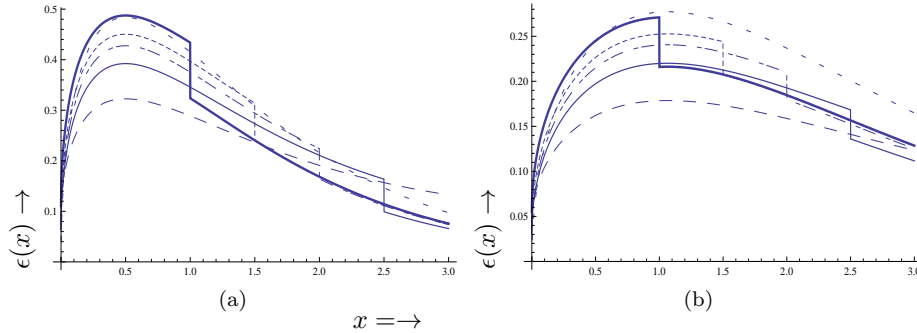


Figure 4.5: The frequency distribution function $g(x) \rightarrow (1 - \epsilon)g(x) + \epsilon g_{df}(x)$ with respect to the galaxy (a) and in the local frame (b). The top line corresponds to $g(x)$ only. Otherwise from top to bottom the lines correspond to $\epsilon = 0.220, 0.222, 0.241, 0.323$ and 0.508 .

- In the local frame:

$$\delta x = (3.06, 3.23, 3.28, 3.23, 2.96) \text{ for } \epsilon = (0.220, 0.222, 0.241, 0.323, 0.508) \text{ respectively}$$

The modulation of the width is exhibited in Fig. 4.6. The width expected in directional experiments is shown in Fig. 4.7.

4.2. The case of caustic rings

Our study of the phase space structure of the Milky Way halo is motivated in large part by the ongoing searches for dark matter on Earth, using axion, see e.g. [14, 11], and WIMP detectors, see e.g. [30, 31, 32, 33, 34]. The signal in such detectors depends on the velocity distribution of dark matter in the solar neighborhood. The caustic ring halo model predicts, see e.g. [28], that most of the local dark matter is in discrete flows and provides the velocity vectors and densities of the first forty flows at the Earth's location in the Galaxy, which are essential when interpreting a signal in a dark matter detector on Earth. In principle the halo model can be treated as phase-mixed DM leading to a linear combination of a M-B distribution and one appropriate to caustic rings, in a fashion similar to that with debris flow discussed above. We will, however, concentrate here in caustic rings.

The relevant information for our purposes can be extracted from table V of Duffy and Sikivie [28], which has improved and updated earlier versions, and

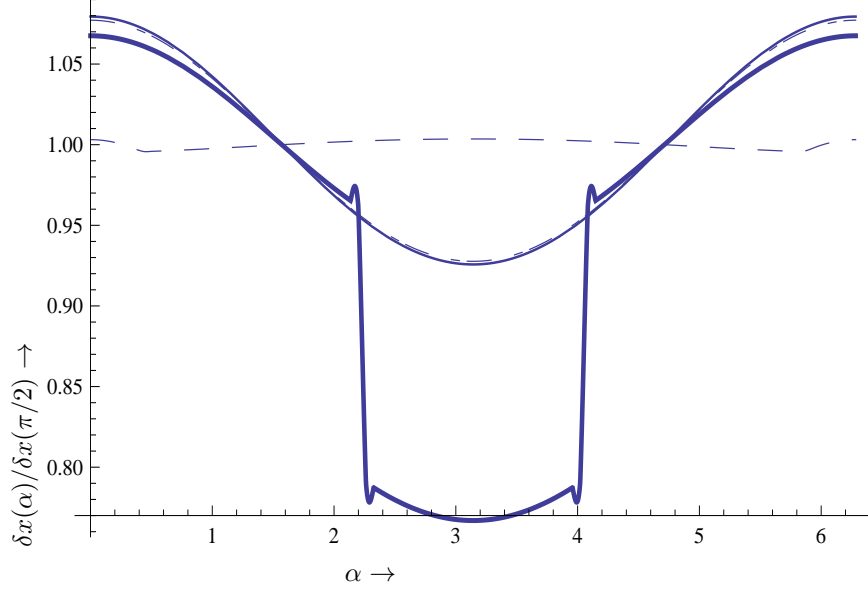


Figure 4.6: The modulated width, relative to its time average, as a function of the phase of the Earth for various values of ϵ . $\epsilon = 0.220, 0.222, 0.241, 0.323, 0.508$ is associated with thick solid, dotted, dot-dashed, fine solid and dashed lines respectively. The dotted and the fine solid lines cannot be resolved.

for the reader's convenience is summarized in table 4.1. One then writes the velocity distribution as

$$\begin{aligned}
 f(v_z) &= \sum_{n\pm} \eta_{v_\phi^{n\pm}} \delta(v_z - v_\phi^{n\pm}), \\
 f(v_x) &= \sum_{n\pm} \eta_{v_\rho^{n\pm}} \delta(v_x - v_\rho^{n\pm}), \\
 f(v_y) &= \sum_{n\pm} \eta_{v_z^{n\pm}} \delta(v_y - v_z^{n\pm})
 \end{aligned} \tag{4.18}$$

where v_x, v_y, v_z are the components of the velocity components in our notation. $\eta_{v_\phi^{n\pm}}, \eta_{v_\rho^{n\pm}}, \eta_{v_z^{n\pm}}$ are suitable normalization factors extracted from the corresponding densities of the last columns of table 4.1. With these ingredients we compute the modulated widths, see Fig. 4.8. We observe that the difference between the maximum and the minimum is 0.08. Note, however, that the maximum is shifted from $\alpha = 0$ (June third) $\alpha = 0.79\pi$, i.e. to approximately

Table 4.1: The velocities caustic ring velocities in our vicinity of our galaxy. The components are given in Sikivie's notation. In our notation for the galactic axes we use $\hat{\phi} \rightarrow \hat{z}, \hat{\rho} \rightarrow \hat{x}, \hat{z} \rightarrow \hat{y}$

| n | $v^{n\pm}$ km/s | $v_{\phi}^{n\pm}$ km/s | $v_z^{n\pm}$ km/s | $v_{\rho}^{n\pm}$ km/s | d_n^+ 10^{-26}gr/cm^3 | d_n^- 10^{-26}gr/cm^3 |
|-----|--------------------|---------------------------|----------------------|---------------------------|-------------------------------------|-------------------------------------|
| 1 | 650 | 140 | ± 635 | 0 | 0.3 | 0.3 |
| 2 | 600 | 250 | ± 540 | 0 | 0.8 | 0.8 |
| 3 | 565 | 380 | ± 420 | 0 | 1.9 | 1.9 |
| 4 | 540 | 440 | ± 310 | 0 | 3.4 | 3.4 |
| 5 | 520 | 505 | 0 | ± 120 | 150. | 15. |
| 6 | 500 | 430 | 0 | ± 260 | 6.0 | 3.1 |
| 7 | 490 | 360 | 0 | ± 330 | 3.9 | 1.2 |
| 8 | 475 | 325 | 0 | ± 350 | 1.9 | 1.0 |
| 9 | 460 | 265 | 0 | ± 375 | 1.4 | 0.7 |
| 10 | 450 | 220 | 0 | ± 390 | 0.9 | 0.9 |
| 11 | 440 | 200 | 0 | ± 390 | 0.8 | 0.8 |
| 12 | 430 | 180 | 0 | ± 390 | 0.7 | 0.7 |
| 13 | 420 | 170 | 0 | ± 390 | 0.6 | 0.6 |
| 14 | 415 | 155 | 0 | ± 385 | 0.6 | 0.6 |
| 15 | 405 | 140 | 0 | ± 380 | 0.5 | 0.5 |
| 16 | 400 | 13 | 0 | ± 375 | 0.5 | 0.5 |
| 17 | 390 | 120 | 0 | ± 370 | 0.5 | 0.5 |
| 18 | 380 | 110 | 0 | ± 365 | 0.4 | 0.4 |
| 19 | 375 | 100 | 0 | ± 360 | 0.4 | 0.4 |
| 20 | 370 | 95 | 0 | ± 355 | 0.4 | 0.4 |

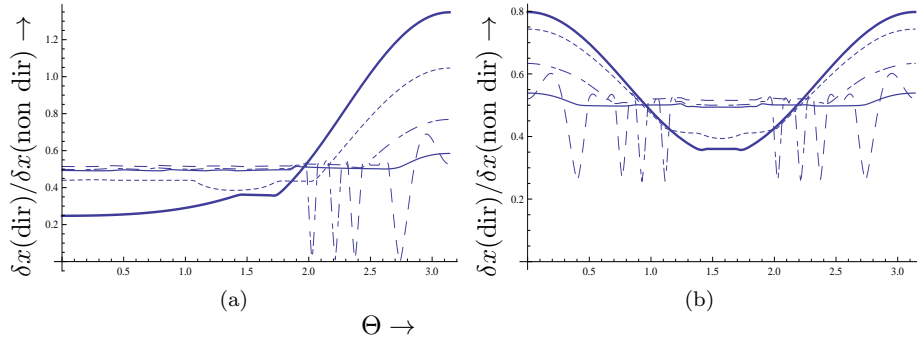


Figure 4.7: The width δx expected in directional experiments, relative to that expected in standard experiments, as a function of the angle between the direction of observation and the sun’s direction of motion, in the presence of debris flows. The exhibited results correspond to the two cases: The sense of direction is known (a) or is not determined (b). Otherwise the notation is the same as in Fig. 4.6. We see that the effect of the debris flows is to decrease δx in all directions.

two weeks later. This is expected due to the asymmetries in the caustic velocity distribution. We also have obtained the directional dependence of the width, see Fig. 4.9. We note, however, that in this case the width depends on the azimuthal angle Φ . This does not occur in the case of symmetric velocity distributions so long as the velocity of the Earth is neglected. Here the variation can be sizable for directions of observation lying in a plane perpendicular to the sun’s velocity, but small away from it. This is another special signature of the caustic ring scenario. Anyway in this case one need not know the sense of direction of the axion.

5. Discussion

In the present work we discussed the time variation of the width of of the axion to photon resonance cavities involved in Axion Dark Matter Searches, by considering a number of popular halo models. We find two important signatures:

- Annual variation due to the motion of the Earth around the sun. We find that in the relative width, i.e. the width divided by its time average, can attain significant differences between the maximum expected in June and the minimum expected six months later. This variation is larger than the modulation expected in ordinary dark matter of WIMPs. It does not

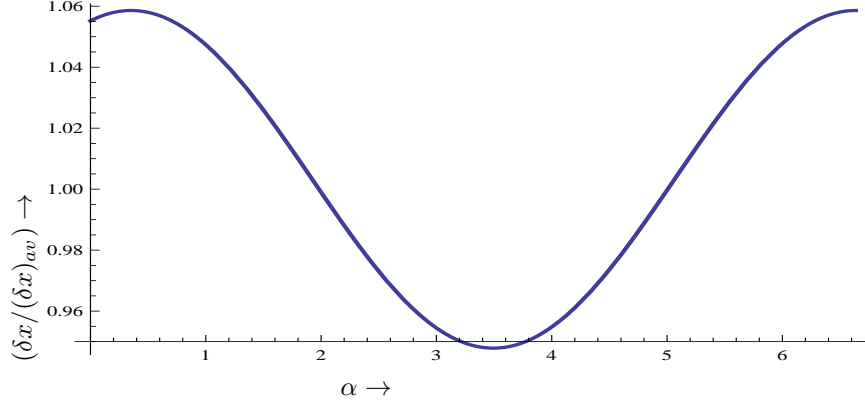


Figure 4.8: The width modulated width δx relative to the time averaged width expected in the case of caustic rings. Note that in this case the maximum does not occur at $\alpha = 0$, but a bit later.

depend on the geometry of the cavity or other details of the apparatus. It depends somewhat on the assumed velocity distribution.

- The width depends strongly of the angle of direction of observation relative to the sun's direction of motion, even if the sense of direction is not known. This can manifest itself as a characteristic diurnal variation due to the rotation of the Earth around its own axis (see our earlier work [16] on how one can translate the directional data into diurnal variation). Anyway once such a device is operating, data can be taken as usual. Only one has to bin them according the time they were obtained. If a potentially useful signal is found, a complete analysis can be done according the directionality to firmly establish that the signal is due to the axion.

In conclusion in this work we have elaborated on two signatures that might aid the analysis of axion dark matter searches. Eventually, if such an observation is made, one may be able to exploit the results obtained here to gain information about the velocity distribution associated with the various halo models.

References

- [1] R. Peccei, H. Quinn, Phys. Rev. Lett 38 (1977) 1440.
- [2] S. Weinberg, Phys. Rev. Lett. 40 (1978) 223.
- [3] F. Wilczek, Phys. Rev. Lett. 40 (1978) 279.

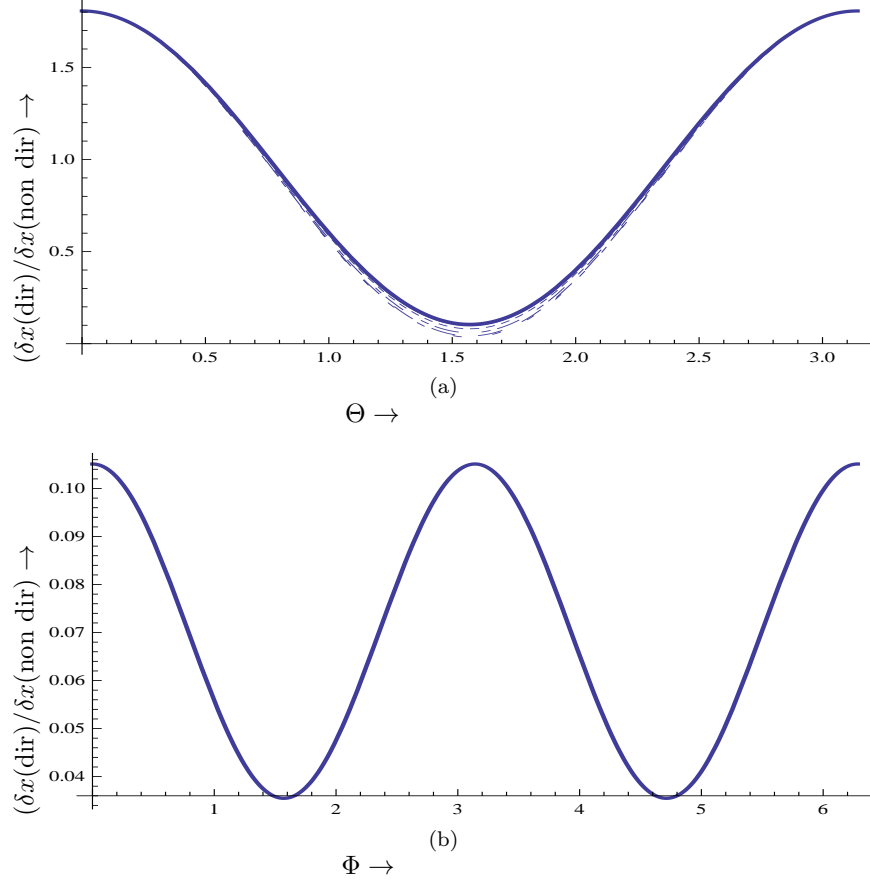


Figure 4.9: The width δx expected in directional experiments, relative to that of the standard (non directional experiments), as a function of the angle between the direction of observation and the sun's direction of motion for various values of Φ (a). The Φ dependence, expected due to the asymmetries of the caustic ring distribution, is quite small. We also show the Φ dependence if the direction of observation is made in a plane perpendicular to the sun's direction of motion (b)

. The effect is now small.

- [4] J. Preskill, M. B. Wise, F. Wilczek, Phys. Lett. B120 (1983) 127.
- [5] L. F. Abbott, P. Sikivie, Phys. Lett. B120 (1983) 133.
- [6] M. Dine, W. Fischler, Phys. Lett. B120 (1983) 137.

- [7] J. Primack, D. Seckel, B. Sadoulet, *Ann. Rev. Nuc. Par. Sc.* 38 (1988) 751.
- [8] P. Sikivie, *Phys. Rev. Lett.* 51 (1983) 1415.
- [9] I. P. Stern, *ArXiv* 1403.5332 (2014) physics.ins-det, on behalf of ADMX and ADMX-HF collaborations, Axion Dark Matter Searches.
- [10] G. Rybka, The Axion Dark Matter Experiment, IBS MultiDark Joint Focus Program WIMPs and Axions, Daejeon, S. Korea October 2014.
- [11] S. J. Asztalos, et al., *Phys. Rev. Lett.* 104 (2010) 041301, the ADMX Collaboration, *arXiv:0910.5914* (astro-ph.CO).
- [12] A. Wagner, et al., *Phys. Rev. Lett.* 105 (2010) 171801, for the ADMX collaboration; *arXiv:1007.3766* (astro-ph.CO).
- [13] Center for Axion and Precision Physics research (CAPP), Daejeon 305-701, Republic of Korea. More information is available at <http://capp.ibs.re.kr/html/capp-en/>.
- [14] S. J. Asztalos, et al., *Nucl. Instr. Meth. in Phys. Res. A* 656 (2011) 39, *arXiv:1105.4203* (physics.ins-det).
- [15] G. Raffelt, Astrophysical Axion Bounds , IBS MultiDark Joint Focus Program WIMPs and Axions, Daejeon, S. Korea October 2014.
- [16] Y. Semertzidis, J.D. Vergados, *Nuc. Phys. B* 897 (2015) 821, *arXiv:1412.6907* (hep-ph).
- [17] Y. Semertzidis and J. D. Vergados, Proceedings of the 18th International Conference: From the Planck Scale to the Electroweak Scale 25-29 May 2015 Ioannina, Greece, *arXiv:1511.08516* (astro-ph.GA).
- [18] Y. H. Ahn, Flavored Peccei-Quinn symmetry, *arXiv:1410.1634* [hep-pj].
- [19] J. Hong, J. E. Kim, S. Nam, Y. Semertzidis, *arXiv:1403.1576* (2014) physics.ins-det, calculations of Resonance enhancement factor in axion-search tube experiments.
- [20] J. E. Kim, *Phys. Rev. D* 58 (1998) 055006.
- [21] L. Krauss, J. Moody, F. Wilczek, D. Morris, *Phys. Rev. Lett.* 55 (1985) 1797.
- [22] L. Duffy, et al., *Phys. Rev. Lett.* 95 (2005) 09134, for the ADMX Collaboration.
- [23] L. Duffy, et al., *Phys. Rev. D* 74 (2006) 012006, for the ADMX Collaboration.

- [24] J. Vergados, Phys. Rev. D. 85 (2012) 123502, ; arXiv:1202.3105 (hep-ph).
- [25] M. Kuhlen, M. Lisanti, D. Spergel, Phys. Rev. D 86 (2012) 063505, arXiv:1202.0007 (astro-ph.GA).
- [26] P. Sikivie, Phys. Rev. D 60 (1999) 063501.
- [27] P. Sikivie, Phys. Lett. B 432 (1998) 139.
- [28] L. D. Duffy, P. Sivie, Phys. Rev. D 78 (2008) 063508.
- [29] J. D. Vergados, Phys. Rev. D 63 (2001) 063511.
- [30] E. Aprile, et al., Phys. Rev. Lett. 107 (2011) 131302, arXiv:1104.2549v3 [astro-ph.CO].
- [31] R. Bernabei, et al., Int. J. Mod. Phys A 28 (2013) 1330022, doi: 10.1142/S0217751X13300226.
- [32] E. Armengaud, et al., Phys. Lett. B 702 (2011) 329, arXiv:1103.4070v3 [astro-ph.CO].
- [33] D. Akerib, et al., Phys. Rev. Lett. 96 (2006) 011302, arXiv:astro-ph/0509259 and arXiv:astro-ph/0509269.
- [34] K. Abe, et al., Astropart. Phys. 31 (2009) 290, arXiv:v3 [physics.ins-det]0809.4413v3 [physics.ins-det].